J. metamorphic Geol., 2002, **20,** 697–708

An automated strategy for calculation of phase diagram sections and retrieval of rock properties as a function of physical conditions

J. A. D. CONNOLLY AND K. PETRINI
Earth Sciences Department, Swiss Federal Institute of Technology, 8092 Zurich, Switzerland (james.connolly@erdw.ethz.ch)

ABSTRACT We formulate an algorithm for the calculation of stable phase relations of a system with constrained bulk composition as a function of its environmental variables. The basis of this algorithm is the approximate representation of the free energy composition surfaces of solution phases by inscribed polyhedra. This representation leads to discretization of high variance phase fields into a continuous mesh of smaller polygonal fields within which the composition and physical properties of the phases are uniquely determined. The resulting phase diagram sections are useful for understanding the phase relations of complex metamorphic systems and for applications in which it is necessary to establish the variations in rock properties such as density, seismic velocities and volatile-content through a metamorphic cycle. The algorithm has been implemented within a computer program that is general with respect to both the choice of variables and the number of components and phases possible in a system, and is independent of the structure of the equations of state used to describe the phases of the system.

Key words: phase diagram; pseudosection; rock properties; seismic velocity: thermodynamics.

INTRODUCTION

Traditionally petrologists have relied on phase diagram projections that implicitly show phase relations for all possible compositions of a system as an explicit function of environmentally determined thermodynamic potentials (see Appendix for nomenclature). The utility of this projection, i.e. a petrogenetic grid, that normally represents only one-dimensional univariant phase fields, is that it constrains the maximum stability of any possible phase assemblage irrespective of the bulk composition of the system. Unfortunately, interpretation of such diagrams is complex in that there may be many assemblages that are stable within any given region of the diagram, and only a small subset of the depicted phase relations may be relevant for a specified composition. Moreover, if the phases of the system are solutions, it is to be expected that for a given composition, high variance fields rather than the univariant fields of the conventional petrogenetic grid will limit phase stabilities. Phase diagram sections computed for a specified bulk composition offer an alternative to projections that avoid these complexities. Following recent geological usage (e.g. Powell, 1978), we designate such sections as pseudosections. In contrast to projections, there is only one state represented by any point within a pseudosection, so that at each point the composition and proportions of the phases and the thermodynamic properties of the system are uniquely determined. While the value of pseudosections is recognized in the geological literature, techniques for the construction of pseudosections are laborious. In this paper we present a strategy for the construction of pseudosections from thermodynamic data. The essence of this strategy is the discretization of the continuous fields of a pseudosection by a polygonal mesh. The phase relations of the polygonalized section are easily interpreted, and, because properties such as volatile contents or density are associated with the polygons, the diagrams provide a simple means of retrieving rock and mineral properties as a function of environmental conditions.

The value of pseudosections as a tool for interpreting petrological equilibria has been amply demonstrated (e.g. Powell & Holland, 1988; Dymoke & Sandiford, 1992; Xu *et al.*, 1994). Because pseudosections provide a map of both mineral chemistry and modes as a function of environmental variables they have application in thermobarometry (e.g. Stuewe & Powell, 1995); where, compared to conventional inverse modelling thermobarometric techniques, phase diagram based methods have the advantage of thermodynamic consistency (e.g. Connolly *et al.*, 1994). The efficacy of phase diagram methods has been limited by the requirement of a complete thermodynamic model for the solution phases of interest; however, efforts to expand data compilations (e.g. Berman &

© Blackwell Science Inc., 0263-4929/02/$15.00

Aranovich, 1996; Gottschalk, 1997; Holland & Powell, 1998) have made substantial progress toward overcoming this limitation. A fundamental caveat in the application of pseudosections to petrological problems is that it is necessary to define an effective thermodynamic bulk composition (e.g. Stuewe, 1997). In many natural systems, there is no meaningful effective bulk composition because disequilibrium fractionation continuously modifies the composition of the equilibrated portion of the rock in response to environmental factors. Where it can be argued that disequilibrium is not important, a second complication in the use of pseudosections is that their geometries can be sensitive to uncertainties in the composition of interest. Thus, thermobarometric applications require an efficient means by which this sensitivity can be explored; the method discussed here is a tool for this exploration.

Perhaps the most important application of pseudosections is that they provide a practical model for the average behaviour of rocks in metamorphic systems. While such models may appear crude to petrologists, they are essential for understanding many geological processes. Past applications of this ilk have focused on physical models of the metamorphic process (e.g. Trommsdorff & Connolly, 1996; Stuewe & Powell, 1997; Connolly, 1997; Kerrick & Connolly, 1998; Guiraud *et al.*, 2001) or the influence of phase transitions on geophysical or geodynamic models (e.g. Saxena & Eriksson, 1983; Wood & Holloway, 1984; Gubbins *et al.*, 1994; Sobolev & Babeyko, 1994; Bina, 1998). Recent applications of both types (e.g. Jull & Kelemen, 2001; Kerrick & Connolly, 2001a,b; Petrini *et al.*, 2001; Lucassen *et al.*, 2001; Muntener *et al.*, 2001; Cesare *et al.*, 2002) demonstrate the effectiveness of the computer method presented here.

Several completely or partially automated computer strategies for the calculation of petrological phase equilibria are widely used by geologists. We begin by reviewing these strategies to clarify the merits of the techniques and to provide the motivation for our modification. Then our strategy is presented in detail and concludes with a demonstration of its computer implementation, in which the phase relations of a metapelite are calculated as a function of pressure (P) and temperature (T). For simplicity, we adopt terminology appropriate for the analysis of an isobaric-isothermal closed chemical system. In this case the Gibbs energy is the thermodynamic function that is minimized during phase equilibrium calculations, the compositional variables describe the proportions of the different kinds of mass that may vary among the phases of the system, and the environmental variables are pressure and temperature. However, our computational strategy is general and can be used for compositions that define the thermal and mechanical properties and environmental variables that relate to the chemistry (Connolly, 1990).

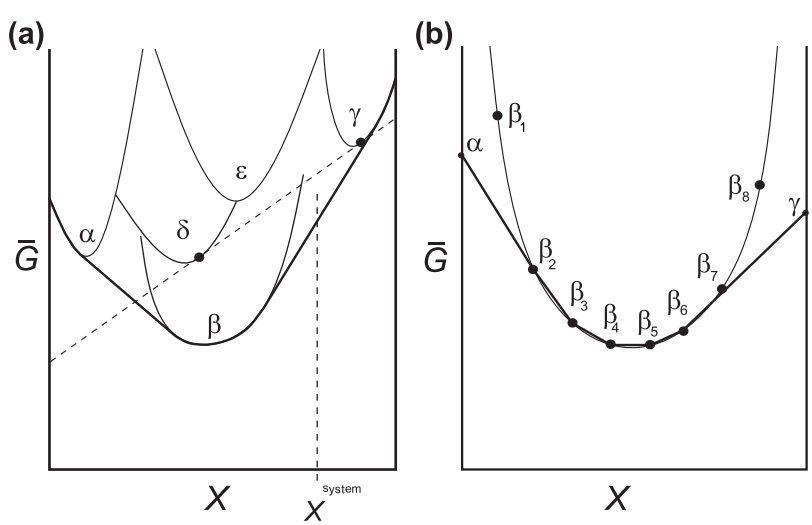

Fig. 1. (a) Schematic isobaric-isothermal $\overline{G} - X$ diagram for a binary system with solution phases (α, β, γ, δ, ε). Minimization strategies (e.g. Saxena & Eriksson, 1983; Wood & Holloway, 1984; De Capitani & Brown, 1987; Eriksson & Hack, 1990) determine the stable assemblage for a specified composition, for example for X^{system} the stable assemblage would be $\beta + \gamma$. Phase equilibrium calculators compute the equilibrium compositions (e.g. Powell *et al.*, 1998; Spear, 1988) of a specified set of coexisting phases. If the assemblage $\delta + \gamma$ is specified, an equilibrium calculator determines the compositions (filled circles) of δ and γ that are tangent to a common $\overline{G} - X$ plane. If these compositions span that of the system, the assemblage is a possible equilibrium in terms of mass balance, but, as illustrated, the assemblage may be metastable. Connolly & Kerrick (1987) developed a strategy that simultaneously determines all the assemblages on the systems minimum $\overline{G} - X$ surface (heavy solid curve). This strategy is efficient if pseudocompounds are used to define the possible compositions of solutions, e.g. in (b) β is represented by pseudocompounds $\beta_1 \ldots \beta_8$, the accuracy of this representation is determined by the pseudocompound spacing.

REVIEW OF EXISTING STRATEGIES

Four basic strategies have been employed for the calculation of pseudosections for petrological applications involving solution phases. The most straightforward strategy is to use a nonlinear free energy minimization technique to map the phase relations of a system as a function of the section variables (e.g. Saxena & Eriksson, 1983; Wood & Holloway, 1984; DeCapitani & Brown, 1987; Sobolev & Babeyko, 1994; Bina, 1998). With this method all the variables of the system are specified and the phase assemblage that minimizes its free energy is computed. To illustrate this procedure consider a molar free-energy ($\overline{G}$) composition (X) diagram for a binary system (Fig. 1a). For the specified composition (X^{system}), minimization establishes the identities, amounts, and compositions of the stable phases ($\gamma + \beta$). By varying pressure or temperature it would then be possible to find conditions at which either one of these phases disappears or a new phase appears, thus defining a pseudosection phase field boundary. Although the calculation of any individual equilibrium with this strategy is done by computer, integration of the results to obtain a pseudosection is time consuming. Attempts to automate this integration have met with some success (Eriksson & Hack, 1990; DeCapitani, pers. comm., 1994), but are not always well suited for the types of problems common in petrology. A technical difficulty in nonlinear minimization problems is convergence to local (false) minima; while many algorithms reduce the probability of this, absolute certainty cannot be assured for systems with nonideal phases.

A second strategy makes use of a phase equilibrium calculator (Powell & Holland, 1988; Powell *et al.*, 1998; see also Hillert, 1981). This strategy is distinguished from free-energy minimization in that the phases of an equilibrium are specified, rather than the variables of the system. Returning to our illustration (Fig. 1a), by this methodology the user might specify the metastable assemblage $\gamma + \delta$. The calculator computes the equilibrium compositions of the coexisting phases, but in contrast to a minimization technique does not test the stability of the assemblage. The calculator can also determine whether the assemblage is possible for a composition of the system, and if it is, the environmental conditions at which one phase in the equilibrium vanishes. These conditions may define a phase field boundary in a pseudosection. Because phase field boundaries can be located directly, rather than by the iterative procedures, the technique offers some advantages over free-energy minimization. Spear (1988) advocates a third strategy by which the changes in the phases of a stable equilibrium are determined as a function of environmental variables by application of the Gibbs–Duhem relation. As with the Holland and Powell strategy, this methodology can be used to determine conditions when a phase disappears from a system due to homogeneous equilibration in response to changing environmental conditions. Because these techniques do not directly establish the stability of equilibria, construction of a phase diagram section by these methods is labour intensive and requires *a priori* knowledge of phase stabilities. The recognition of phase immiscibility also creates technical complications for equilibrium calculators because the calculators solve systems of equations that are formulated in terms of phase species, rather the phases themselves.

We focus on a fourth strategy in which the systems minimum free energy surface is determined directly (i.e. the heavy solid curve in Fig. 1a; Connolly & Kerrick, 1987; Greiner, 1988). The result of such a computation is identical to that which would be obtained by energy minimization computations repeated for all possible compositions of a system, or alternatively by establishing the stability of all possible equilibria in a system through the use of a phase equilibrium calculator. Once these phase relations are known, mass balance constraints can be used to establish which equilibrium is relevant for a particular composition, and the phase relations of this equilibrium can be monitored as a function of environmental variables to obtain the desired phase diagram section. It is not to be expected that this strategy will in general be superior to iterative application of a minimization technique. However, the efficiency of this strategy increases enormously if the continuous compositional variation of solutions is represented by a series of discrete compositions, i.e. discretized (Connolly & Kerrick, 1987). The initial implementation of this strategy as a component of a computer program called VERTEX (Connolly, 1990) has had application for the calculation of pseudosections (e.g. Gubbins *et al.*, 1994; Trommsdorff & Connolly, 1996; Connolly, 1997; Kerrick & Connolly, 1998), but was complicated by two problems that we resolve here. First, to maximize efficiency, Connolly & Kerrick (1987) made use of geometric constraints that required substantial computer memory and thereby limited the dimension and resolution of the compositional space that could be treated. Here a simpler and more general algorithm is introduced that overcomes these limitations. The second problem is that VERTEX defines phase diagrams by identifying the conditions at which changes in the stable phase assemblages occur rather than by identifying the assemblages themselves. While this is desirable for the construction of petrogenetic grids where the stability fields of phase assemblages may overlap, it results in a loss of information in the context of a pseudosection. To recover this information we adopt an algorithm whereby pseudosections are subdivided into polygonal regions that correspond to phase fields.

COMPOSITIONAL DISCRETIZATION: PSEUDOCOMPOUND APPROXIMATION

The free energy surface of a solution phase is a nonlinear function of its composition and consequently the

numerical solution of phase equilibrium problems is complicated. To circumvent such complications, Connolly & Kerrick (1987) suggested an approximation by which the compositional variation of a solution is represented by a series of compounds defined such that each compound has the thermodynamic properties of the solution at an arbitrarily chosen composition. To distinguish these compounds from true phases, the compounds are designated pseudocompounds. This approximation is illustrated for a binary system with three possible phases (Fig. 1b), where α and γ are true compounds, and β is a solution represented by the pseudocompounds $\beta_1 \ldots \beta_8$. After the approximation the true curvilinear minimum $\overline{G} - X$ surface the system, which defines both the stable phase assemblages and the possible compositions of the stable phases, becomes a piecewise linear hull defined by the vertices α, $\beta_2, \ldots, \beta_6$, γ (the heavy segmented curve in Fig. 1b). More generally, in a c-component system, at arbitrarily specified environmental conditions, the approximated minimum $\overline{G} - X$ surface of the system is a convex faceted $c - 1$ dimensional surface, each facet of which is defined by c compounds that stably coexist. The true variance of the assemblage corresponding to any facet can be established by counting the number of phases represented by the compounds. Thus, $\alpha + \beta_2$ and $\beta_6 + \gamma$ are two-phase assemblages, whereas assemblages such as $\beta_2 + \beta_3$ represent a portion of the homogeneous one-phase region of solution β. Immiscibility is recognized by testing whether two, or more, coexisting pseudocompounds of a solution bound the composition of a metastable pseudocompound of the same solution. For example, stability of the assemblage $\beta_2 + \beta_7$ would imply the existence of a solvus in β spanning the compositions $\beta_3, \ldots, \beta_6$.

The distinction between apparent and true variance of phase assemblages approximated by pseudocompounds is also useful in characterizing changes in the phase relations of a system as a function of environmental variables. Returning to our illustration (Fig. 1b), if the solution β is destabilized with respect to the compounds α and γ in response to a change in some environmental variable, then this destabilization must be manifest by a discontinuous reaction of the form $\beta_2 = \beta_3 + \alpha$ or $\beta_6 = \beta_5 + \gamma$. The equilibrium of such a reaction has an apparent variance of one (i.e. the equilibrium is pseudounivariant), but because the same phase appears twice in the reaction the true variance of the phase assemblage represented by the reaction is two. In a phase diagram projection or section, the conditions of these pseudounivariant equilibria define isopleths of the solution β in the divariant fields of the assemblages $\alpha + \beta$ or $\beta + \gamma$. In the context of this example, the ultimate stability of the solution β would be associated with a reaction of the form $\beta_4 = \alpha + \gamma$, this reaction is recognized as univariant because each compound represents a distinct phase. In contrast to the true univariant field, for which the associated reaction stoichiometry changes continuously, the variation in the reaction stoichiometry for the approximated univariant field occurs discontinuously at pseudoinvariant fields defined by an assemblage such as $\beta_4 + \beta_5 + \alpha + \gamma$.

The essence of the pseudocompound approximation is that in a pseudosection defined by two environmental variables, any two-dimensional phase field must represent the stability field of an assemblage consisting of c compounds and therefore has an apparent variance of two. Pseudodivariant phase fields are separated by one-dimensional univariant fields that intersect to define zero-dimensional invariant fields. The true variance of these fields is determined by counting the number of phases represented by the fields, or, in the special case of phase immiscibility, by applying a geometric test. These procedures can be done within the same computer program that is used to establish the phase fields. Thus, pseudocompounds are an internal representation and both input and output to programs based on the algorithm can be expressed in terms of continuous solution phases and true variance. The accuracy of the approximation is determined by the compositional spacing of the pseudocompounds, given current computational resources this is not an important limitation for geological problems. Various schemes (e.g. Connolly & Kerrick, 1987) for the internal generation of pseudocompounds are described in the program documentation.

STABLE PHASE ASSEMBLAGES AS A FUNCTION OF COMPOSITION

In this section, an abbreviated combinatorial algorithm to establish the stable phase assemblages of a system as a function of its composition at constant, and arbitrarily chosen, environmental conditions is developed. For the purposes of the algorithm there is no distinction between true compounds and pseudocompounds, so discussion is simplified by the assumption that all possible phases are true compounds. Gibbs' conditions require that for the equilibrium of p compounds the chemical potentials of each component, in every compound in which it occurs, must be equal. From the definition of the Gibbs energy, this condition is expressed

$$\sum_{j=1}^{c} X_j^i \mu_j = \overline{G}^i, \quad i = 1, \ldots, p \tag{1}$$

where i indexes the properties of the compounds. If the Gibbs energies and compositions of the compounds are known, then eq. (1) is a system of p linear equations in c unknowns. It follows, that all, and only, assemblages of $p = c$ compounds with linearly independent compositions uniquely define the equilibrium states of the system. Such assemblages are stable if the condition:

$$\overline{G}^i - \sum_{j=1}^{c} X_j^i \mu_j \geq 0 \quad i = 1, \ldots, \pi \tag{2}$$

is true for the π compounds possible in the system. Based on these constraints, we formulate an algorithm consisting of an initial step in which a stable compound assemblage is identified. New assemblages involving a subset of $c - 1$ compounds of the assemblage(s) already known to be stable are identified in the second step. This step is repeated using the assemblages identified in the previous iteration as seeds until no new assemblages are identified and the composition diagram is completely determined. In detail, the structure of each step is:

Step 1. The stable phase in a one-component subcomposition is found. Components are progressively added to the subcomposition, and after each addition, the compound that stably coexists with the compounds known to be stable from the previous step is determined. When all c components have been included, the assemblage of c compounds is a stable divariant assemblage that defines a corner on the simplicial hull of the systems minimum $\overline{G} - X$ surface.

Step 2. Each $c - 1$ compound permutation of the c-compound assemblages identified in the previous step is examined to determine if the permutation is not present in any other stable assemblage identified in the current or previous step. If this condition is met, then a compound is sought that lies on the opposite side of the $c - 1$ dimensional plane spanning the compositions of the permutation from the compound already known to coexist with the permutation. If such a compound exists, then there is an additional stable assemblage involving the permutation. The compound is then taken as an initial guess for the compound that coexists with the permutation and eq. (1) is solved. The stability of this new assemblage is tested by eq. (2), if the assemblage is found to be metastable with respect to the jth phase, the guess for the stable phase is updated to be the jth phase, and eq. (2) is evaluated for the remaining $\pi - j$ phases. The assemblage identified in this manner is stable, but may duplicate an assemblage already identified in the same iteration. Thus the assemblage must be compared to a list of assemblages identified in the current step.

To illustrate this procedure consider the ternary system shown in Fig. 2. In the initial step of the algorithm the stable compound, α, in the subcomposition defined by component 1 is identified; the subcomposition is expanded to include component 2, and the stable compound, γ, that coexists with α in the binary, is established. The subcomposition is then augmented to the full ternary composition, and the compound, β_3, that coexists with the $\alpha + \gamma$ is found. For the second step, the assemblage is $\alpha + \gamma + \beta_3$ is now known to be stable; therefore there are two stable $c - 1$ phase permutations to be considered $\alpha + \beta_3$ and $\gamma + \beta_3$ that may coexist with a third compound ($\alpha + \gamma$ is excluded *a priori* because it lies in a subcomposition and therefore must be on the edge of the composition space). Beginning with $\alpha + \beta_3$, the compounds β_4, β_5 and β_6 lie on the opposite side of the line (i.e. a $c - 1$ dimensional plane) spanning the compositions of $\alpha + \beta_3$ from the compound γ and therefore may coexist with $\alpha + \beta_3$. One of these compounds is chosen to form a trial configuration, such as $\alpha + \beta_3 + \beta_6$, for which eq. (1) is solved. The stability of β_4 and β_5 is then tested relative to the trial configuration with eq. (2), if either of these compounds is found to be stable relative to the trial configuration the compound replaces β_6 in the trial configuration, and the stability of the new trial configuration is tested against the remaining compounds. The procedure for the second permutation, $\gamma + \beta_3$, is identical except that this assemblage may only coexist with the compounds β_4, β_5, β_6 and δ. If a trial configuration is not metastable with respect to any of the compounds with which it may coexist, then it is accepted as a stable assemblage.

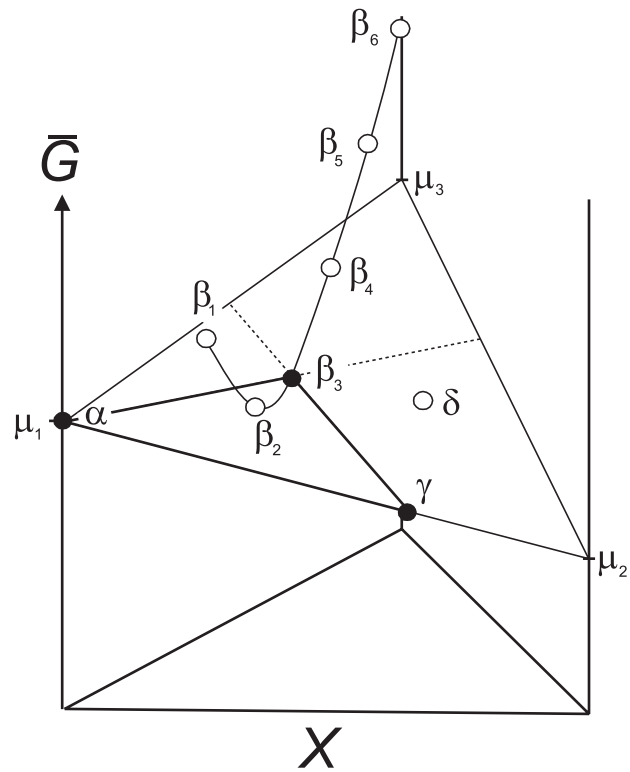

Fig. 2. Schematic isobaric-isothermal $\overline{G} - X$ diagram for a ternary system illustrating the unconstrained minimization strategy used in VERTEX. From eq. (1), any assemblage of $p = c$ compositionally nondegenerate compounds defines a $\overline{G} - X$ plane. The assemblage is stable if there are no compounds with $\overline{G} - X$ co-ordinates below this plane (eq. 2) is true as is the case for the assemblage $\alpha + \gamma + \beta_3$ (open circles indicate compounds that lie above the $\alpha + \gamma + \beta_3$ $\overline{G} - X$ plane). In the initial step of the algorithm the stable compound, α, in the subcomposition defined by component 1 is identified; the subcomposition is expanded to include component 2, and the stable compound, γ, which coexists with α in the binary, is established. With the addition of the third component to the composition space, the stable compound β_3 that coexists with the binary assemblage $\alpha + \gamma$ is identified. In the second step, phases are sought that coexist with every permutation of c–1 compounds from the assemblage(s) identified in the previous step.

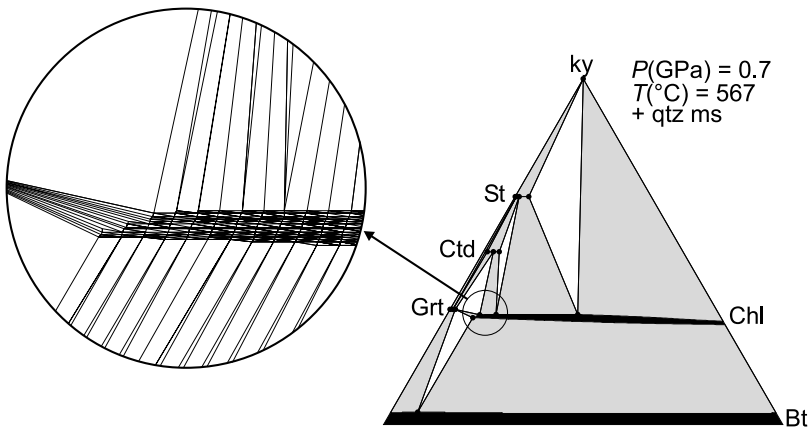

Fig. 3. AFM diagram illustrating the capacity of the program VERTEX to provide high resolution of compositional phase relations, thermodynamic data as discussed in reference to Fig. 5, mineral notation after Kretz (1983) with stoichiometric phases indicated by lower case abbreviations. Inset shows phase relations in terms of the pseudocompounds specified for the calculation. Calculation and drafting, which required < 5 s on a 200-MHz computer, was done using > 20000 pseudocompounds. Reconstruction of true phase relations is done automatically by the graphics program PSVDRAW.

If at the conclusion of this step, the stable configurations identified in this manner are $\alpha + \beta_3 + \beta_4$ and $\gamma + \beta_3 + \beta_4$, then in the next iteration of this step there are again two stable $c - 1$ phase permutations to be considered $\alpha + \beta_4$ and $\gamma + \beta_5$ (here $\beta_3 + \beta_4$ is excluded *a priori* because it is common to two stable assemblages). The calculation is concluded when all the stable $c - 1$ phase assemblages identified are either common to two assemblages or cannot coexist with any of the compounds possible in the system (i.e. they are on the edge of the portion of the composition space that can be physically realised given the compounds defined for the problem).

As a demonstration of the practicality of the foregoing algorithm, Fig. 3 shows a calculated 'AFM' diagram (Thompson, 1957) in which the compositions of two ternary and nine binary solutions are resolved to an accuracy of one percent. The computer time required to calculate and draft the diagram is less than five seconds on a computer with a clock speed of 200 MHz.

Extension to constrained bulk composition

The algorithm outlined above determines all the stable compound assemblages of a system irrespective of its composition. Excepting cases of pathological degeneracy, only one of these assemblages will be stable for a given bulk composition. Discounting the caveat, this assemblage is identified by determining the proportions α_i of the compounds in each assemblage necessary to obtain the systems composition by solving the mass balance constraint:

$$\sum_{j=1}^{p} X_j^i \alpha_i = X_j^{\text{system}}, \quad j = 1, \ldots, c \qquad (3)$$

The stable compound assemblage is that assemblage for which the proportions of the compounds are greater than zero.

For most purposes, pseudosections are used for problems in which the amounts of all the components are specified, i.e. the rank of Eqs. 2 and 3 is c. However, under some circumstances it may be desirable to constrain only a subset of the systems components, e.g. a situation where the Fe:Mg ratio of a system is known, but the proportions of the remaining components cannot be defined. Alternatively, it may be desirable to reduce the dimension of the composition space by specifying that one or more components are present in excess. In VERTEX, multiple component saturation constraints are implemented by a component saturation hierarchy; a scheme that preserves thermodynamic consistency and permits thermodynamic projections through solution phases (Connolly, 1990). In these cases, the rank of eq. (3) is greater than that of eq. (1). As there is no algorithmic constraint on the rank of eq. (3), these situations are easily dealt with using the foregoing algorithm.

POLYGONALIZED PHASE DIAGRAM SECTIONS

As a consequence of the pseudocompound approximation, the maximum apparent variance of any phase assemblage is two and thus the stability of these assemblages can only be limited by either univariant fields or invariant fields where univariant fields intersect. To establish the conditions for these low variance fields we employ the following algorithm, illustrated in Fig. 4, for a system with a fully constrained composition; for partially constrained compositions we employ the algorithm outlined by Connolly (1990).

Step 1. The stable divariant assemblage is determined, by the procedure outlined previously, at an arbitrary point along the boundary of the pseudosection co-ordinate frame ($\alpha + \gamma$ at point a, Fig. 4).

Step 2. One co-ordinate frame variable is incremented until the divariant assemblage becomes metastable with respect to exactly one compound (β_1 at conditions immediately beyond point b, Fig. 4). This compound together with the initial assemblage comprises the assemblage of the univariant field. The univariant field is located on the edge of the co-ordinate frame by solving for the equilibrium condition of the relevant univariant reaction ($\alpha + \gamma = \beta_1$ at point b, Fig. 4; see also Eqs. A1 and A2, Appendix).

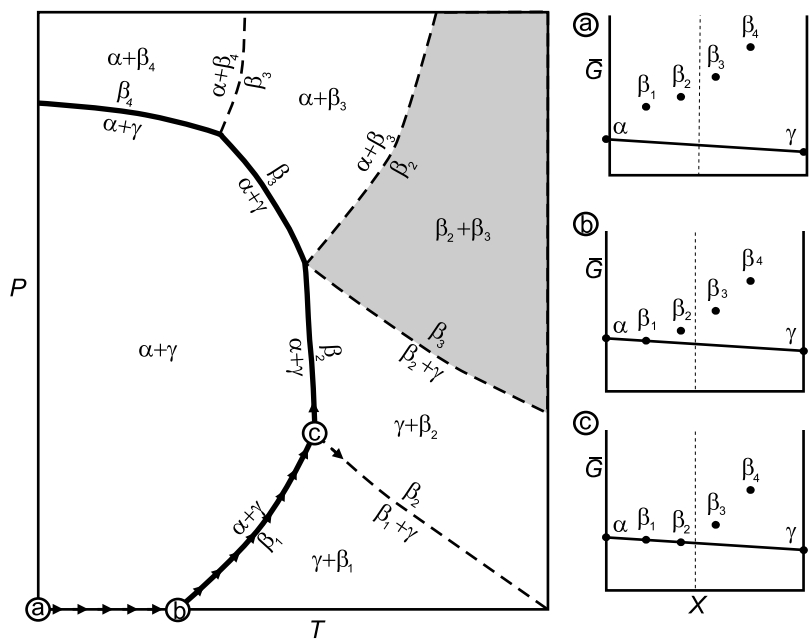

Fig. 4. Schematic pseudosection for a binary system illustrating the tracing algorithm used by VERTEX. Arrows indicate the path traced by VERTEX, with $\overline{G} - X$ diagrams at points along the path as discussed in the text. In the $\overline{G} - X$ diagrams, the vertical dashed line indicates the systems composition. One-dimensional univariant fields are traced by locating conditions at which $c + 1$ phases are simultaneously tangent to a $\overline{G} - X$ plane subject to the condition that there are no other compounds below the plane, as in (b); univariant fields may terminate at zero-dimensional invariant fields located by conditions at which an additional compound becomes tangent to the $\overline{G} - X$ plane of the univariant field. The divariant fields separated by each univariant field are established by finding the two c-phase permutations of the univariant assemblage that span the composition of the system (eq. 3). The univariant fields divide the P–T space of the section into a polygonal mesh, the program POLYGON assembles this mesh from the output generated by VERTEX and associates a divariant assemblage with each polygon, e.g. the field $\beta_1 + \beta_2$ (shaded) constitutes one element of the mesh. True phase field variance is determined by counting the number of phases represented by the compounds; thus, truly univariant phase fields such as $\alpha + \gamma = \beta_1$ are distinguished from pseudounivariant $\beta_1 + \gamma = \beta_2$ fields. Likewise, the programs recognize that two or more elements of the polygonal mesh, such as $\gamma + \beta_1$ and $\gamma + \beta_2$, may represent a single true phase field.

Step 3. The univariant field is traced within the co-ordinate frame, by incrementing one section variable and solving for the other, until it either becomes metastable at an invariant field ($\alpha + \gamma + \beta_1 + \beta_2$ at point c, Fig. 4) or intersects the edge of the co-ordinate frame. In the former case, the additional stable univariant fields that emanate from the invariant field ($\alpha + \gamma + \beta_2$ and $\alpha + \beta_1 + \beta_2$) are established by determining the $c + 1$ phase permutations of the invariant assemblage that span the bulk composition (eq. 3) and these are traced in the same manner. This step is repeated to determine all the univariant fields that connect to the initial univariant field via invariant fields.

If the foregoing procedure is repeated for every divariant field identified on the perimeter of the sections co-ordinate frame, then all the univariant fields relevant to the bulk composition are established. Each of these fields separates two divariant fields, the identities of which are found by determining the two c phase permutations that span the bulk composition (eq. 3). This information completes the definition of the pseudosection, but the interpretation of the pseudosection is complicated by the fact the output of the algorithm defines the edges of the two-dimensional regions of the pseudosection rather than the two-dimensional regions themselves. To eliminate this difficulty we make use of the fact there is a unique divariant assemblage in every two-dimensional field of the pseudosection. Each of these fields is a polygon, the vertices of which correspond to the points along the bounding univariant fields and associated invariant fields or intercepts with the co-ordinate frame where these univariant fields terminate. The program POLYGON assembles this polygonal mesh from the output created by VERTEX and associates a divariant assemblage with each element of the mesh. For our example (Fig. 4), the output from POLYGON would be a mesh consisting of six elements representing the divariant fields $\alpha + \gamma$, $\gamma + \beta_1$, $\gamma + \beta_2$, $\beta_2 + \beta_3$, $\alpha + \beta_3$ and $\alpha + \beta_4$. If it is acknowledged that $\beta_1 \ldots \beta_4$ represent a single solution β, then four true phase fields can be reconstructed from the internal pseudocompound representation: the divariant field $\alpha + \gamma$; the one phase trivariant field of β represented by the pseudodivariant assemblage $\beta_2 + \beta_3$; and the divariant fields of $\gamma + \beta$ and $\alpha + \beta$ represented by divariant assemblages $\{\gamma + \beta_1, \gamma + \beta_2\}$ and $\{\alpha + \beta_3, \alpha + \beta_4\}$, respectively. For graphical purposes the true phase relations are obtained with the program PSVDRAW. In its default mode PSVDRAW shows all true univariant fields

(e.g. $\alpha + \beta_1 + \gamma$) and any pseudounivariant fields ($\gamma + \beta_2 + \beta_3$ and $\alpha + \beta_2 + \beta_3$) that define the limit of a true phase region, and suppresses pseudounivariant fields that correspond to boundaries between polygons that represent the same true phase assemblage ($\gamma + \beta_1 + \beta_2$ and $\alpha + \beta_3 + \beta_4$).

To illustrate the tractability of geological problems by our method, the computer implementation of this strategy was applied to the calculation of the phase relations for Shaw's (1956) average metapelite composition (atomic proportions 6.32 Na: 7.12 K: 2.21 Ca: 5.73 Mg: 9.05 Fe: 24.00 Al: 210.14 Si). To constrain the proportions of H_2O, CO_2 and O_2, the system is assumed to be in equilibrium with a fluid formed by equilibration of water with graphite, a model argued to provide a reasonable model for metapelite devolatilization (Connolly & Cesare, 1993). The calculation was made with the thermodynamic data of Holland & Powell (1998), taking into account the crystalline solutions as detailed in Table 1. Computer time required to calculate and draft the pseudosection is *c*. 10 min on a 200-MHz computer. The raw output from VERTEX that forms the basis of the polygonalized pseudosection is shown in Fig. 5(a); the section after processing with POLYGON is shown in Fig. 5(b), with labelling suppressed for legibility; and the final redrafted section is shown in Fig. 5(c). The computed phase relations are consistent with petrographic observation (e.g. Bucher & Frey, 1994), an agreement that provides some assurance that current thermodynamic models are adequate for modelling natural systems. Discretization of solution composition limits the resolution of certain pseudosection features, most notably in Fig. 5(c) this is manifest in the narrow high variance fields that separate phase fields of lower variance and uncertainty as to the arrangement of high variance phase fields about the ends of univariant fields. Examples of this uncertainty are the small triangular trivariant fields that terminate the univariant field that limits the stability of albite with respect to plagioclase (at *c*. 450 °C, 0.7 GPa in Fig. 5c). While the existence of these fields cannot be rejected on the basis of topological arguments, their small size leads to the suspicion that they are an artefact of compositional discretization. The validity of such features can usually be verified by refining the discretization scheme, but in some cases unambiguous resolution requires numerically exact computational procedures (e.g. those of Powell *et al*., 1998 or Spear, 1989).

Table 1. Mineral solution notation, formulae and model sources (1 = Holland & Powell, 1998; 2 = modified from Anovitz & Essene, 1987; 3 = Holland *et al*., 1998; 4 = modified from modified from Gasparik, 1985 and Holland & Powell, 1998; 5 = Thompson & Waldbaum, 1969; 6 = modified from Chatterjee & Froese, 1975 and Holland & Powell, 1998; 7 = Newton *et al*., 1980). The compositional variables *w*, *x*, *y*, and *z* may vary between zero and unity and are determined as a function of pressure and temperature by free-energy minimization.

Symbol	Solution	Formula	Source
Amph	amphibole	$Ca_{2-2z}Na_zMg_xFe_{(1-x)}Al_{3w+4y}Si_{8-2w-2y}O_{22}(OH)_2$	1
Bio	biotie	$KMg_{(3-y)x}Fe_{(3-y)(1-x)}Al_{1+2y}Si_{3-y}O_{10}(OH)_2$	1
Cal	calcite	$Ca_{1-x-y}Mg_xFe_yCO_3$	2
Chl	chlorite	$Mg_{(5-y+z)x}Fe_{(5-y+z)(1-x)}Al_{2(1+y-z)}Si_{3-y+z}O_{10}(OH)_8$	3
Cph	carpholite	$Mg_xFe_{1-x}Al_2Si_2O_6(OH)_4$;	1
Cpx	clinopyroxene	$Na_{1-y}Ca_yMg_{xy}Fe_{(1-x)y}Al_ySi_2O_6$	4
Crd	cordierite	$Mg_{2x}Fe_{2-2x}Al_4Si_5O_{18}\cdot(H_2O)_y$	1
Ctd	chloritoid	$Mg_xFe_{1-x}Al_2SiO_5(OH)_2$	1
Dol	dolomite	$CaMg_xFe_{1-x}(CO_3)_2$	1
Ep	epidote	$Ca_2Al_{3-2x}Fe_{2x}Si_3O_{12}OH$	1
Gl	glaucophane	$Ca_{2-2z}Na_zMg_xFe_{1-x}Al_{3w+4y}Si_{8-2w-2y}O_{22}(OH)_2$	1
Grt	garnet	$Fe_{3x}Ca_{3y}Mg_{31-x-y}Al_2Si_3O_{12}$	1
Kfs	alkali feldspar	$Na_xK_yAlSi_3O_8$	5
Mgs	magnesite	$Mg_xFe_{1-x}CO_3$	1
Ms	muscovite	$K_xNa_{1-x}Mg_{yw}Fe_{(1-y)w}Al_{3-2w}Si_{3+w}O_{10}(OH)_2$	6
Ol	olivine	$Mg_xFe_{1-x}SiO_4$	1
Opx	orthopyroxene	$Mg_{x(2-y)}Fe_{(1-x)(2-y)}Al_{2y}Si_{2-y}O_6$	1
Pl	plagioclase	$Na_xCa_{1-x}Al_{2-x}Si_{2+x}O_8$	7
Pg	paragonite	$K_xNa_{1-x}Mg_{yw}Fe_{(1-y)}Al_{3-2w}Si_{3+w}O_{10}(OH)_2$	6
Prg	amphibole	$Ca_2Na_wMg_xFe_{1-x}Al_{3w+4y}Si_{8-2w-2y}O_{22}(OH)_2$	1
Sa	sanidine	$Na_xK_yAlSi_3O_8$	5
Sp	spinel	$Mg_xFe_{1-x}AlO_3$	1
St	staurolite	$Mg_{4x}Fe_{4-4x}Al_{18}Si_{7.5}O_{48}H_4$	1

Once a polygonalized pseudosection has been computed, chemical and thermophysical properties at any condition within the section are retrieved by the program WERAMI. WERAMI determines the polygonal element spanning the condition of interest and reports the requested properties, a program with similar structure is used by Spear (1999) to recover phase diagram information. Because of the pseudocompound approximation, mineral chemistry changes only across the boundaries of the polygonal elements of the pseudosection, whereas thermophysical properties vary both continuously through a polygonal element and discontinuously across its boundary. These properties can be visualized directly as a false colour image by assigning representative values to each element of the polygonal mesh. Alternatively, property values can be sampled on a grid or path, defined by an arbitrary polynomial, through the pseudosection and then interpolated to provide a continuous model for the properties. This latter mode of representation is used to depict modal variation of the mineralogy and water content (Fig. 5d) and plagioclase and garnet compositions (Fig. 5e) for our model pelite as a function of pressure and temperature. The latter plot (Fig. 5e) demonstrates that when the use of pseudosections is justified, mineral solution chemistry provides an extraordinarily simple thermobarometric method. The irregular trajectories of the mineral isopleths are due to abrupt changes in the *P–T* dependence of mineral composition across phase field boundaries.

PRACTICAL IMPLEMENTATION OF THE ALGORITHM

The programs VERTEX, POLYGON and WERAMI are components of a collection of FORTRAN computer programs for the calculation and graphical representation of phase equilibria. This package, including documentation, can be copied via Internet (http://www.perplex.ethz.ch). This web site also includes a tutorial

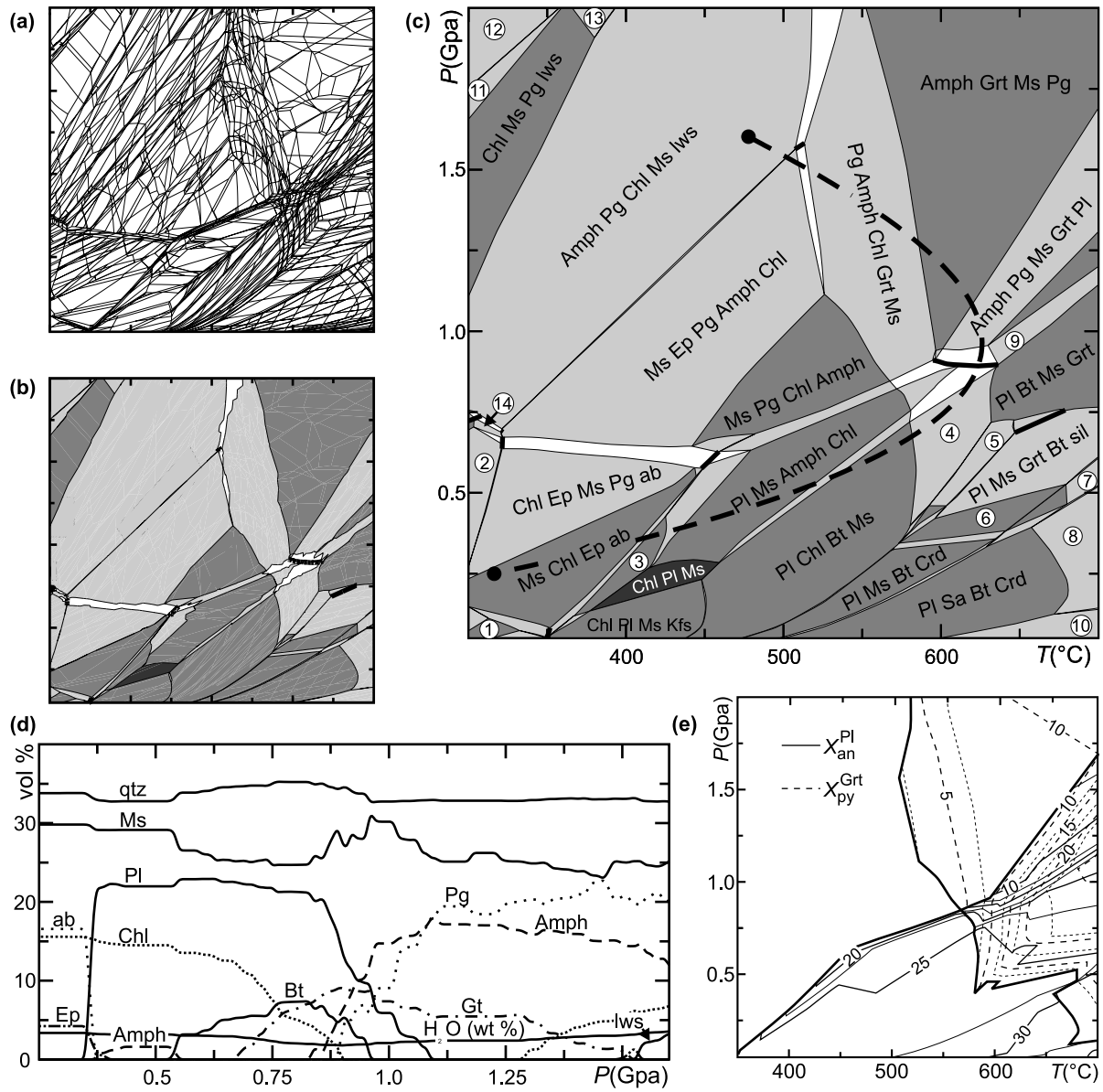

Fig. 5. Computed pseudosection for Shaw's (1956) average (subaluminous) metapelite composition, solution models as in Table 1, compositions were resolved with minimum accuracy of 3 mol percentage. Calculation and drafting required *c*. 10 min on a 200-MHz computer. Raw output from VERTEX (a) consists of pseudounivariant curves; this output is processed by Polygon to obtain the pseudosection (b, labels omitted for legibility), which is redrafted in (c). Univariant fields shown by heavy solid lines, divariant fields by white fill, and higher variance fields by progressively darker shading. All fields include quartz in addition to the indicated mineralogy. Numbered fields in (c) correspond to: (1) ab + Chl + Ms + wrk (wairakite), (2) ab + Cal + Chl + Ms + Pg, (3) Chl + Ep + Ms + Pl, (4) Bt + Chl + Grt + Ms + Pl, (5) Bt + Grt + Ms + Pl + St, (6) Bt + Ms + Pl + sil, (7) Bt + Grt + Pl + Sa + sil, (8) Bt + Crd + Grt + Pl + sil, (9) Amph + Bt + Grt + Ms + Pl, (10) Bt + Crd + Ol + Pl + Sa, (11) Chl + Crp (carpholite) + lws + Ms + Pg, (12) Chl + Cpx + Crp + lws + Ms, (13) Chl + Cpx + lws + Ms + Pg, (14) Amph + Cal + Chl + Ms + Pg. Unlabelled phase fields can be deduced from the rule that adjacent phase fields differ by only one phase. (d) Modal variations, along path indicated by heavy dashed curve in (c). (e) Contour plot of the mole fractions of the anothite end-member in plagioclase and the pyrope end-member in garnet, heavy solid curves indicate stability fields of plagioclase and garnet. Both (d) and (e) constructed from the polygonalized pseudosection by WERAMI.

outlining the steps necessary for the computation illustrated by Fig. 5. The programs can be used with most recent geological thermodynamic databases (e.g. Johnson *et al.*, 1992; Berman & Aranovich, 1996; Gottschalk, 1997; Holland & Powell, 1998). Because the FORTRAN sources of the programs are available, the programs can be modified to accommodate mineral equations of state that have not been anticipated in the

present code or for other specialized purposes. Graphical output from the package is written in interpreted PostScript that can be imported into commercial graphical editors.

DISCUSSION

The advance accomplished by this work is technical in that we have developed a robust and general method for computing pseudosections that requires no *a priori* knowledge of the phase relations in question. Our method eliminates several difficulties endemic to numerically exact nonlinear optimization strategies; these problems include convergence to local (metastable) free energy minima; numerical instability; and, in the case of equilibrium calculators, complications caused by phase separation. Additionally, the approach advocated here offers a more rational means of representing the computed phase relations than can be obtained by conventional energy minimization strategies (e.g. Saxena & Eriksson, 1983; Wood & Holloway, 1984; DeCapitani & Brown, 1987; Eriksson & Hack, 1990). In contrast to the methods outlined by Powell *et al*. (1998) and Spear (1988), the approach has the advantage that of being fully automated. The feasibility of our strategy rests on the discretization of the continuous compositional variation of solution phases with pseudocompounds (Connolly & Kerrick, 1987). While discretization results in finite accuracy, it is unlikely that this is a major limitation given present computational resources and accuracy of mineralogical solution models. In cases where this assumption proves untrue, our approach may serve as a complement to numerically exact procedures.

ACKNOWLEDGEMENTS

We are grateful to F. Spear and R. White for constructive reviews and to R. Powell for his editorial comments and suggestions. Y. Podladchikov, A. Barnicoat and D. Kerrick provided the impetus for this work, which was supported by US National Science Foundation MARGINS program.

REFERENCES

Anovitz, L. & Essene, E. J., 1987. Phase equilibria in the system $CaCO_3$-$MgCO_3$-$FeCO_3$. *Journal of Petrology*, **28,** 389–414.

Berman, R. G. & Aranovich, L. Y., 1996. Optimized standard state and solution properties of minerals. I. Model calibration for olivine, orthopyroxene, cordierite, garnet and ilmenite in the system FeO-MgO-CaO-Al_2O_3-TiO_2-SiO_2. *Contributions to Mineralogy and Petrology*, **126,** 1–24.

Bina, C. R., 1998. Free energy minimization by simulated annealing with applications to lithopsheric slabs and mantle plumes. *Pure and Applied Geophysics*, **151,** 605–618.

Bucher, K. & Frey, M., 1994. *Petrogenesis of Metamorphic Rocks*. Springer, Berlin.

Cesare, B., Marchesi, C. & Connolly, J. A. D., 2002. Growth of myrmekite coronas by contact metamorphism of granitic mylonites in the aureole of Cima di Vila (Eastern Alps – Italy). *Journal of Metamorphic Geology*, **20,** 203–213.

Chatterjee, N. D. & Froese, E., 1975. A thermodynamic study of the pseudo-binary join muscovite-paragonite in the system $KAlSi_3O_8$-$NaAlSi_3O_8$-Al_2O_3-SiO_2-H_2O. *American Mineralogist*, **60,** 985–993.

Connolly, J. A. D., 1990. Multivariable phase diagrams: an algorithm based on generalized thermodynamics. *American Journal of Science*, **290,** 666–718.

Connolly, J. A. D., 1997. Devolatilization-generated fluid pressure and deformation-propagated fluid flow during regional metamorphism. *Journal of Geophysical Research*, **102,** 18149–18173.

Connolly, J. A. D. & Cesare, B., 1993. C-O-H-S fluid composition and oxygen fugacity in graphitic metapelites. *Journal of Metamorphic Geology*, **11,** 379–388.

Connolly, J. A. D. & Kerrick, D. M., 1987. An algorithm and computer program for calculating composition diagrams. *CALPHAD*, **11,** 1–54.

Connolly, J. A. D., Memmi, I., Trommsdorff, V., Franceshelli, M. & Ricci, C. A., 1994. Forward modeling of calc-silicate microinclusions and fluid evolution in a graphitic metapelite (NE Sardinia). *American Mineralogist*, **79,** 960–972.

DeCapitani, C. & Brown, T. H., 1987. The computation of chemical equilibria in complex systems containing non-ideal solutions. *Geochimica Cosmochimica Acta*, **51,** 2639–2652.

Dymoke, P. & Sandiford, M., 1992. Phase relationships in Buchan Facies series pelitic assemblages: calculations with application to andalusite-staurolite parageneses in the Mount Lofty Ranges, South Australia. *Contributions to Mineralogy and Petrology*, **110,** 121–132.

Eriksson, G. & Hack, K., 1990. Chemsage – a computer program for the calculation of complex chemical equilibria. *Metallurgical Transactions B*, **21B,** 1013–1023.

Gasparik, T., 1985. Experimental study of subsolidus phase relations and mixing properties of pyroxene and plagioclase in the system Na_2O-CaO-Al_2O_3-SiO_2. *Contributions to Mineralogy and Petrology*, **89,** 346–357.

Gottschalk, M., 1997. Internally consistent thermodynamic data for rock forming minerals. *European Journal of Mineralogy*, **9,** 175–223.

Greiner, H., 1988. Computing complex chemical equilibria by generalized linear programming. *Mathematical and Computer Modelling*, **10,** 592–650.

Gubbins, D., Barnicoat, A. & Cann, J., 1994. Seismological constraints on the grabbro-eclogite transition in subducted oceanic crust. *Earth and Planetary Science Letters*, **122,** 89–101.

Guiraud, M., Powell, R. & Rebay, G., 2001. H_2O in metamorphism and unexpected behaviour in the preservation of metamorphic mineral assemblages. *Journal of Metamorphic Geology*, **19,** 445–454.

Hillert, M., 1981. A discussion of methods for calculating phase diagrams. *Bulletin of Alloy Phase Diagrams*, **2,** 265–268.

Hillert, M., 1985. A review of phase diagram principles. *International Metallurgical Reviews*, **30,** 45–65.

Holland, T., Baker, J. & Powell, R., 1998. Mixing properties and activity-composition relationships of chlorites in the system MgO-FeO-Al_2O_3-SiO_2-H_2O. *European Journal of Mineralogy*, **10,** 395–406.

Holland, T. J. B. H. & Powell, R., 1998. An internally consistent thermodynamic data set for phases of petrological interest. *Journal of Metamorphic Geology*, **16,** 309–343.

Johnson, J. W., Oelkers, E. H. & Helgeson, H. C., 1992. SUPCRT92: a software package for calculating the standard molal thermodynamic properties of minerals, gases, aqueous species, and reactions from 1 to 5000 bar and 0–1000°C. *Computers and Geosciences*, **18,** 899–947.

Jull, M. & Kelemen, P. B., 2001. On the conditions for lower crustal convective instability. *Journal of Geophysical Research*, **106,** 6423–6446.

Kerrick, D. M. & Connolly, J. A. D., 1998. Subduction of ophicarbonates and recycling of CO_2 and H_2O. *Geology*, **26,** 375–378.

Kerrick, D. M. & Connolly, J. A. D., 2001a. Metamorphic devolatilization of subducted marine sediments and transport of volatiles to the Earth's mantle. *Nature*, **411,** 293–296.

Kerrick, D. M. & Connolly, J. A. D., 2001b. Metamorphic devolatilization of subducted oceanic metabasalts: implications for seismicity, arc magamatism and volatile recycling. *Earth and Planetary Science Letters*, **189,** 19–29.

Kretz, R., 1983. Symbols for rock-forming minerals. *American Mineralogist*, **68,** 277–279.

Lucassen, F., Becchio, R., Harmon, R. *et al*. 2001. Composition and density model of the continental crust at an active continental margin – the Central Andes between 21° and 27°S. *Tectonophysics*, **341,** 195–223.

Muntener, O., Kelemen, P. B. & Grove, T. L., 2001. The role of H_2O during crystallization of primitive arc magmas under uppermost mantle conditions and genesis of igneous pyroxenites: an experimental study. *Contributions to Mineralogy and Petrology*, **141,** 643–658.

Newton, R. C., Charlu, T. V. & Kleppa, O. J., 1980. Thermochemistry of the high structural state plagioclases. *Geochemica Cosmochimica Acta*, **44,** 933–941.

Palatnik, L. S. & Landau, A. I., 1964. *Phase Equilibria in Multicomponent Systems*. Holt, Rinehart and Winston, Inc, New York.

Petrini, K., Connolly, J. A. D. & Podladchikov, Y., 2001. A coupled petrological-tectonic model for basin evolution: The influence of metamorphic reactions on the tectonic subsidence of sedimentary basins. *Terra Nova*, **13,** 354–359.

Powell, R., 1978. *Equilibrium Thermodynamics in Petrology: an Introduction*. Harper & Row, London.

Powell, R. & Holland, T. J. B. H., 1988. An internally consistent thermodynamic dataset with uncertainties and correlations: 3. application to geobarometry worked examples and a computer program. *Journal of Metamorphic Geology*, **6,** 173–204.

Powell, R., Holland, T. J. B. H. & Worley, B., 1998. Calculating phase diagrams involving solid solutions via non-linear equations, with examples using THERMOCALC. *Journal of Metamorphic Geology*, **16,** 577–588.

Saxena, S. K. & Eriksson, G., 1983. Theoretical computation of mineral assemblages in pyrolite and lherzolite. *Journal of Petrology*, **24,** 538–555.

Schmalzreid, V. H. & Pelton, A. D., 1973. Zur geometrischen Darstellung von Phasengleichgewichten. *Bunsengesellschaft Fuer Physikalische Chemie*, **77,** 90–94.

Shaw, D. M., 1956. Geochemistry of pelite rocks III, major elements and general geochemistry. *Geological Society of America Bulletin*, **67,** 919–934.

Sobolev, S. V. & Babeyko, A. Y., 1994. Modeling of mineralogical composition, density, and elastic-wace velocities in anyhdrous magmatic rocks. *Surveys in Geophysics*, **15,** 515–544.

Spear, F. S., 1988. The Gibbs method and Duhem's theorem: The quantitative relationships among P, T, chemical potential, phase composition and reaction progress in igneous and metamorphic systems. *Contributions to Mineralogy and Petrology*, **99,** 249–256.

Spear, F. S., 1999. Real-time AFM diagrams on your Macintosh. *Geological Materials Research*, **1,** 1–18.

Stuewe, K., 1997. Effective bulk composition changes due to cooling: a model predicting complexities in retrograde reaction textures. *Contributions to Mineralogy and Petrology*, **129,** 43–52.

Stuewe, K. & Powell, R., 1995. PT paths inferred from modal proportions. Application to the Koralm Complex, Eastern Alps. *Contributions to Mineralogy and Petrology*, **119,** 83–93.

Stuewe, K. & Powell, R., 1997. Reaction enthalpies of subsolidus equilibria in pelitic rocks. Magnitude and influence on Cretaceous Metamorphism of the Koralm Complex, Eastern Alps. *Mitteilungen Des Naturwissentschaftlichen Vereins der Steirmark*, **127,** 45–60.

Thompson, J. B., 1957. The graphical analysis of mineral assemblages in pelitic schists. *American Mineralogist*, **42,** 842–858.

Thompson, J. B. & Waldbaum, D. R., 1969. Mixing properties of sanidine crystalline solutions. IV. Phase diagrams from equations of state. *American Mineralogist*, **76,** 493–500.

Trommsdorff, V. & Connolly, J. A. D., 1996. The ultramafic contact aureole about the Bregaglia (Bergell) Tonalite: isograds and a thermal model. *Schweizerische Mineralogische Petrographische Mitteilungen*, **76,** 537–547.

Wood, B. J. & Holloway, J. R., 1984. A thermodynamic model for subsolidus equilibria in the system CaO-MgO-Al_2O_3-SiO_2. *Geochimica Cosmochimica Acta*, **66,** 159–176.

Xu, G., Will, T. & Powell, R., 1994. A calculated petrogenetic grid for the system K_2O-FeO-MgO-Al_2O_3-SiO_2-H_2O. *Journal of Metamorphic Geology*, **12,** 99–119.

Received 9 May 2001; revision accepted 6 April 2002.

APPENDIX: PHASE DIAGRAM NOMENCLATURE

Although much of current petrological phase diagram jargon is generally understood, the meaning of some terms is vague. To avoid the possibility that our language gives rise to any ambiguity we review some aspects of phase diagram terminology. The independent variables of phase diagrams can be related to a ratio of extensive properties (e.g. chemical composition), or to an intensive state function (P, T, $\mu_1,\ldots,\mu_c$). Both kinds of variables are intensive and to distinguish them they are designated *potential* (Hillert, 1985; Palatnik & Landau, 1964) and *compositional* (Connolly, 1990) variables, respectively. It is convenient to consider these variables to be the representative co-ordinates of a system composed of c independently variable kinds of matter. A real physicochemical system is *open* with respect to some extensive property if the property may vary through interactions with the environment of the system. These properties must be characterized by potentials, referred to as *environmental* variables, because in equilibrium thermodynamics the nature of such interactions can only be defined if these potentials have the same value both within and beyond the boundaries of the system. The association of the variables of a diagram with the determinative physicochemical properties of a real system is of course unspecified because it is impossible to prescribe the way a phase diagram will be used.

A diagram is a *phase diagram* only if its geometry defines the representative co-ordinates of both a system and its stable phases (e.g. Schmalzreid & Pelton, 1973; Hillert, 1985; Palatnik & Landau, 1964). From the definition of composition variables, it follows that such a diagram must be $c + 1$ dimensional (i.e. only $c + 1$ of the intensive variables can be independent). If all $c + 1$ variables of this diagram are compositions, then diagram is composed of $c + 1$ dimensional *phase fields* that define the loci of conditions for which a specific phase assemblage of p phases is in equilibrium. Defining phase field *variance* as $f \equiv c + 2 - p$, if χ composition variables of the phase diagram are replaced by their conjugate potentials, then the dimension of any phase field with $f < \chi$ is reduced by $\chi - f$ dimensions, because of the equality of potentials among coexisting equilibrium phases.

In general the information in phase diagrams must be presented in two dimensions by sectioning or projection to be of practical value. Phase diagram sections may be defined by potential or composition sectioning variables, and are designated *potential* and *composition sections*, respectively (Hillert, 1985). Potential sections are themselves

phase diagrams because the section defines the state of both the system and its phases. In contrast, composition sections are not phase diagrams because the section defines neither the compositions nor the amounts of the phases. In this respect, usage of the term *pseudosection* to designate composition sections, as implicit in recent geological literature (e.g. Powell *et al.*, 1998), is not inappropriate. We employ the term in this paper as short-hand for composition sections made on a two-dimensional co-ordinate frame defined by two potentials. In this context, $c + 1$ dimensional univariant fields and c dimensional invariant fields appear as curves and points, respectively. It is always possible to write a mass balance relationship, i.e. a *reaction*, among the phases of a univariant field of the general form:

$$\sum_{i=1}^{c+1} \nu^i \vec{\varphi}^i = 0 \tag{A.1}$$

where $\vec{\varphi}^i$ is a vector representing the composition of the ith phase and ν_i is its reaction coefficient. If the potentials of interest are pressure and temperature, a necessary condition for the stability of the univariant assemblage is

$$\sum_{i=1}^{c+1} \nu^i \overline{G}^i = \Delta\overline{G} = 0, \tag{A.2}$$

the sufficient condition being that eq. (1) is true for all nondegenerate permutations of c phases of the univariant assemblage. The reaction coefficients of one, or more, phases in Eq. (A.1) may be zero, thus the reaction equation can be written among a subset of the equilibrium phases, e.g. as would be the case for a polymorphic phase transformation in a system with $c > 1$. We do not follow the common petrological practice of identifying univariant fields by reactions to emphasize that within a univariant field the state of the system can only be defined by all $c + 1$ phases of the fields, regardless of the number of phases involved in the associated reaction. Likewise, we do not follow the practice of identifying univariant and invariant fields as univariant curves and invariant points for two reasons: (i) curves and points represent, by definition, univariant and invariant conditions, and therefore the adjectives are superfluous; and (ii) we seek language that allows concise statement of phase diagram principles such as the *Maessing-Palatnik rule*, which states that adjacent phase fields differ by exactly one phase (e.g. Hillert, 1985).

View publication stats